

THREE-DIMENSIONAL MODELLING AND PARAMETER IDENTIFICATION OF THE SEATED HUMAN BODY EXPOSED TO RANDOM VIBRATION

IGOR MACIEJEWSKI, ANDRZEJ BŁAŻEJEWSKI, SEBASTIAN PECOLT,
TOMASZ KRZYZYNSKI, PIOTR ZAPORSKI

Koszalin University of Technology, Department of Mechatronics and Automation, Koszalin, Poland

e-mail: igor.maciejewski@tu.koszalin.pl; andrzej.blazejewski@tu.koszalin.pl; sebastian.pecolt@tu.koszalin.pl;

tomasz.krzyzynski@tu.koszalin.pl; piotr.zaporski@tu.koszalin.pl

The paper deals with the modelling and parameter identification of the human body in a sitting posture. The advantage of this paper is to announce a simplified, but also a reliable three-mass model representing dynamic behaviour of the main human body parts, i.e. pelvis, torso and head. Their equivalent masses are interconnected by classical mechanical constraints in the form of springs and dampers. The stiffness and damping coefficients are identified by means of an original optimisation procedure that is used to minimise the error between measurement and simulation results. The model is proposed to be used for simulation studies of vibration-induced effects on the human body as well as for defining a specific vibration-isolation properties of automotive seat suspension systems with minimal computing cost and time.

Keywords: bio-mechanical model, human body, vibration exposure

1. Introduction

Bio-mechanical modelling began to develop in the 1970s. Its aim is to replicate the conduct of the human body within a simplified way. Bio-mechanical models can be employed to witness the behaviour of the system in various conditions under the impact of external forces, which enables one to carry out kinetic and dynamic analysis. The main development of bio-mechanical modelling has began in medicine, rehabilitation and sport. At present, bio-mechanical models are widely utilised to predict human interactions with mechanical systems. Computer models of the human body are gaining increasing popularity due to the potential for developing more complicated models that allow study of a given problem on a much larger scale in a much shorter time.

The simplest models, that have been and still are used in study on the system dynamics, are uniaxial models. Despite their simple structure, such systems consist of numerous components and sections along with non-linear properties. Simple uniaxial models are often used to simulate only a selected part of the body in which a single movement direction is dominant. One of the initial bio-mechanical simulations employed for jumping and landing was crafted in the 1980s. The representation portrays the model as a single-axis setup comprised of two masses linked by springs and dampers (Fritz, 1981).

The next stages of development of bio-mechanical models are complex single-axis models for examining the movement of the human physique during diverse undertakings, e.g. contact of the foot against the ground or a three-mass depiction of a seated subject. Two-dimensional models (Liu and Qin, 2020, 2021), with up to several degrees of freedom are additionally employed for investigating kinematics of the human physique. They are used in various sport disciplines

to study specific movements (Maciejewski *et al.*, 2022), for which only individual parts of the human body are modelled. They are also used to carry out analyses covering the entire human body. Such models typically consist of rigid bodies with continuous or discrete weight allocation, frequently regarded as rigid constituents. The advanced programmes enabling analysis of the behaviour of the human model are based on mathematical analysis, are additionally supported by visualization and offer numerous kinematic and dynamic alternatives. They facilitate the construction and simulation of spatial configurations with numerous degrees of liberty. A good illustration is the BoB Biomechanics (Shippen and May, 2016; Mihcin *et al.*, 2019) environment working with MATLAB®.

There are many models that are not directly based on bio-mechanics, which are called virtual computer models (Zhao *et al.*, 2021). A bio-mechanical system like a black box with a specific number of inputs can represent the human interaction and body response outputs. These models do not directly mirror human bio-mechanics, but concentrate on bodily reactions. They are extensively employed in sports (Głowiński *et al.*, 2018), rehabilitation (Głowiński *et al.*, 2017a, 2019), medicine for analysing motion kinematics (Głowiński *et al.*, 2015, 2017b). A lot of research into reducing vibration of seat suspension systems employs bio-mechanical representations of the human physique in a seated stance. Some researchers present complex 3D models with many degrees of freedom (Zheng *et al.*, 2011). Unfortunately, the literature lacks bio-mechanical models of humans that describe human vibration in various directions, even when the input vibration is generated solely along one axis.

Creating a credible human spatial model is not an easy task. In addition to the anthropometric data of the human regarding its individual masses and structural dimensions of the body parts (Chandler *et al.*, 1975), the parameters describing visco-elastic connections (stiffness and damping coefficients) between particular masses are required. The vast majority of these parameters can be identified by using different optimisation techniques. In (Desai *et al.*, 2018), the authors present a 2D multi-body model featuring 20 degrees of freedom (DOF) formulated for a seated subject, with model parameters fine-tuned through the utilisation of a genetic algorithm (GA). The empirical information are achieved from the existing literature (Mandapuram *et al.*, 2011), wherein the biodynamic response to an uncorrelated biaxial vibration is assessed. The impacts of palm support, lumbar cushioning, and vibration intensity on the interplay between the body and the seat and backrest are delineated through the utilisation of the apparent mass concept. The model developed by the authors can replicate the observed seat-to-head transmissibility responses (STHT) of the human physique.

A dependable representation of the human physique enables one to develop the seat suspension system in relation to its vibration isolation characteristics that can improve overall driving comfort of the drivers. There are many studies describing the significance of safeguarding the operator from vertical vibrations experienced in the seat suspension (Stein *et al.*, 2008; Adam and Jalil, 2017), but only a little work is reported on reducing the horizontal vibration (Sun and Jing, 2016; Sun *et al.*, 2015; Maciejewski *et al.*, 2017; Maciejewski and Krzyzyski, 2020). For instance, in the paper (Kim *et al.*, 2005), the authors constructed a bio-mechanical representation of the human physique for evaluating vibrations while in a seated posture. In their work, the model comprises multiple concentrated masses interconnected by linear springs and dampers.

The continuous exposure of the human physique to low-frequency vibration (below 20 Hz) may affect human well-being and comfort. Experimental study of the biodynamic responses of the human physique can aid in comprehending the impacts of vibrations on drivers and as a result to enhance the suspension control strategy. For this purpose, many control methods are employed for enhancement of the operator comfort through semi-active (Maciejewski *et al.*, 2019) and active seat suspension systems (Maciejewski *et al.*, 2022). The aim of this paper is to put forth a bio-mechanical representation of the human physique while seated, which can be

used for simulation studies of the effects of vibration on the drivers and to determine vibration isolation characteristics of automotive seat suspension systems.

2. Physical and mathematical model

A methodology for developing the human model includes the following assumptions. The authors of this paper adopt a strategy aimed at building a minimal model, i.e. as simple as possible and thus computationally efficient. Furthermore, the reliability of this model should be experimentally verified under laboratory conditions. First of all, the physical model of the human body is determined to represent the seated human in a position typical for driving a car, working machine or other motor vehicle (Fig. 1). At this point, it is also decided on the type of coordinate system in which the model is located.

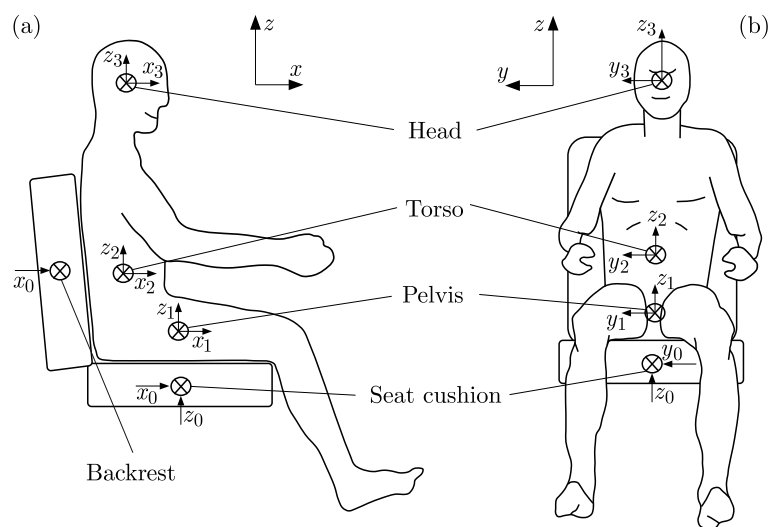


Fig. 1. Posture of the seated human body in a vehicle: (a) side view, (b) front view

In order to simplify the problem formulation and its numerical solution, the three-mass model is considered to represent the human pelvis, torso and head (Fig. 1). Assessing the layout of the human body in the driver's position, Fig. 1 shows two places of the input vibration, e.g. transmitted by the backrest and seat cushion. It is assumed that the driver is mainly influenced by forces transmitted through the seat. The forces acting on the feet and generated by the steering wheel are not taken into account because they are insignificant for the whole-body vibration (WBV) exposure.

2.1. Physical model

Assuming that each mass is a rigid body with finite dimensions (Fig. 2), the anatomical connections between individual parts of the human body are represented by spring-damper systems. Their dynamic properties are defined by appropriate values of the stiffness $k_{i(i-1)j}$ and damping $d_{i(i-1)j}$ coefficients. The indices next to the coefficients indicate the numbers of bodies $i = 1, 2, 3$ between which these systems are placed as well as the direction $j = x, y, z$ in which the spring and damping forces are considered. Due to asymmetrical configuration of the bio-mechanical model, the angular motion of bodies around particular axes is provided and the corresponding torsional stiffness and damping follow from visco-elastic properties of the applied connections. In this model, the locations of the centres of individual bodies are important (symbol *otimes* in Fig. 2), at which kinematic values, i.e. displacements, velocities

and accelerations, are determined. These are linear quantities measured along the xyz coordinate system together with angular quantities θ , φ , ψ that are described around each axis.

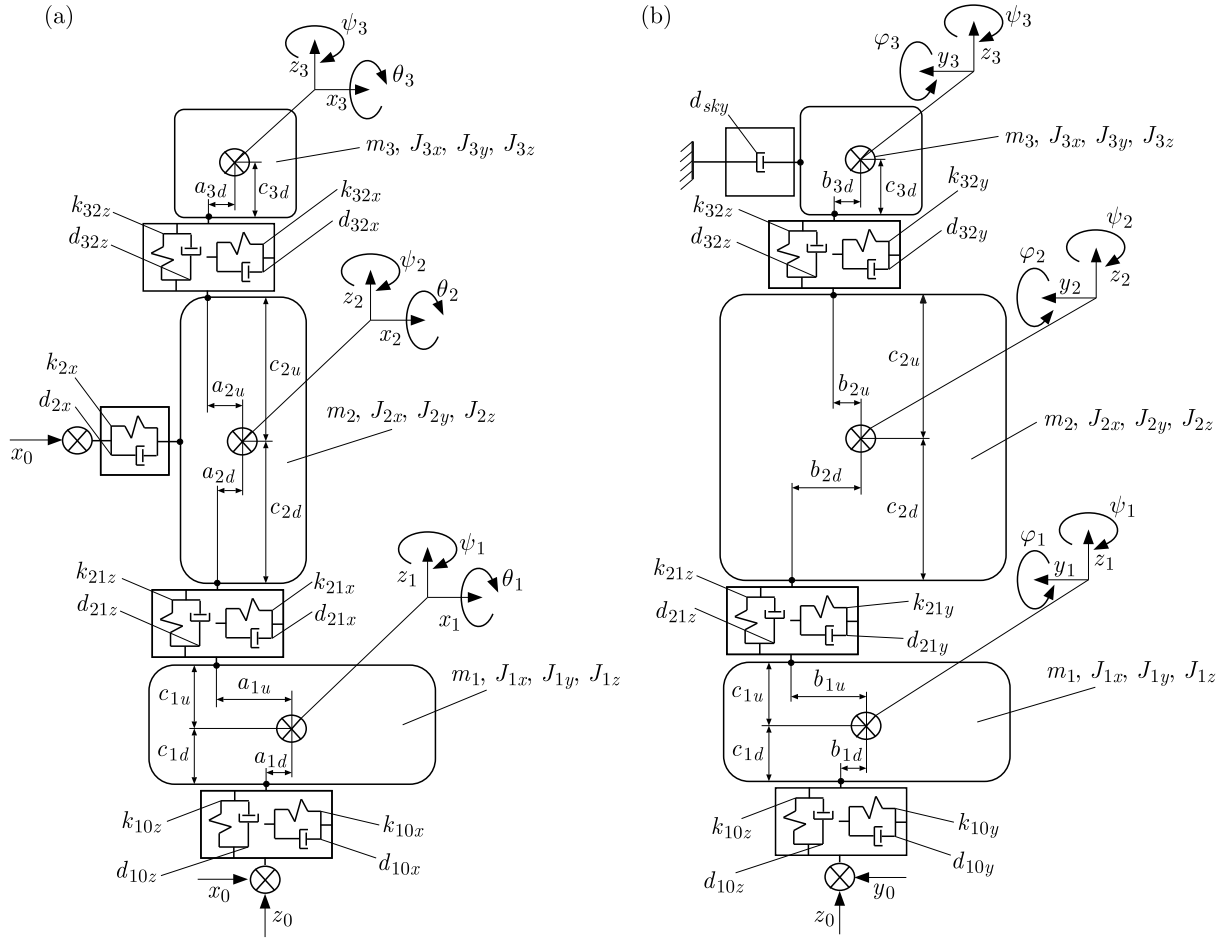


Fig. 2. Physical model of the seated human body: (a) side view, (b) front view

An important feature of aforementioned model is the location of the spring-damper systems in relation to the mass centres. This makes it possible to simulate the behaviour of human body parts, such as head (mass No. 3 in Fig. 2) or torso (mass No. 2 in Fig. 2), whose centres of mass are in fact not aligned (symmetrised) with and pelvis (mass No. 1 in Fig. 2). Possible locations for mounting the visco-elastic elements are defined by their corresponding dimensions, i.e. a_{id} and a_{iu} , b_{id} and b_{iu} , c_{id} and c_{iu} , where the number $i = 1, 2, 3$ represents the selected human body part. The another indexes indicate the mounting position of a given mass, i.e. the indexes u and d mean the upper and lower fixation points, respectively. The physical model presented in this paper (Fig. 2) allows one to develop its mathematical description for the purpose of simulating mechanical reactions of the seated human body to vibration.

2.2. Mathematical model

The mathematical model takes into account linear and angular movements of individual bodies (displacements x_i , y_i , z_i and angles of rotation θ_i , φ_i , ψ_i) that are determined in local coordinate systems with the origins in the centres of each mass (Fig. 3). In this model, the input vibration is transferred through spring-damper elements that are connected at the bottom and top of particular bodies, and these visco-elastic elements generate reaction forces around each axes, i.e. the bottom forces $F_{i(i-1)x}$, $F_{i(i-1)y}$, $F_{i(i-1)z}$ and the top forces $F_{(i+1)ix}$, $F_{(i+1)iy}$, $F_{(i+1)iz}$.

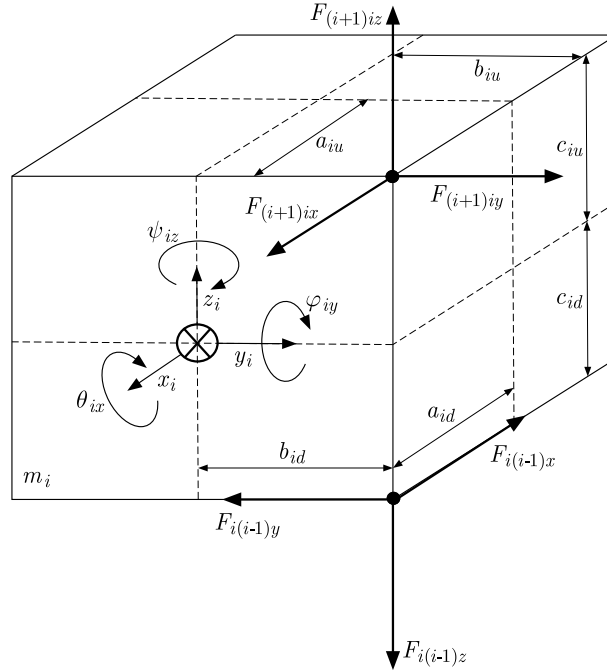


Fig. 3. Forces transferred through spring-damper elements in the local coordinate system of an individual mass

The following equations describe linear motion of particular bodies in different directions

$$\begin{aligned} m_i \ddot{x}_i &= F_{i(i-1)x} + F_{(i+1)ix} + F_{2x} & m_i \ddot{y}_i &= F_{i(i-1)y} + F_{(i+1)iy} + F_{sky} \\ m_i \ddot{z}_i &= F_{i(i-1)z} + F_{(i+1)iz} & i &= 1, 2, 3 \end{aligned} \quad (2.1)$$

where: m_i is mass of individual bodies ($i = 1, 2, 3$), \ddot{x}_i , \ddot{y}_i , \ddot{z}_i are linear accelerations measured along particular axes, F_{2x} is the reaction force of the seat backrest (acting only in the longitudinal x -direction on the torso), F_{sky} is the active force stabilising the human head in the lateral y -direction.

The bottom and top forces connecting individual bodies of the human body model are determined as follows:

— along the x -axis

$$\begin{aligned} F_{i(i-1)x} &= d_{i(i-1)x} [-(\dot{x}_i - \dot{x}_{(i-1)}) - b_{id}(\dot{\psi}_i - \dot{\psi}_{(i-1)}) - c_{id}(\dot{\varphi}_i - \dot{\varphi}_{(i-1)})] + \dots \\ &\quad + k_{i(i-1)x} [-(x_i - x_{(i-1)}) - b_{id}(\psi_i - \psi_{(i-1)}) - c_{id}(\varphi_i - \varphi_{(i-1)})] \\ F_{(i+1)ix} &= d_{(i+1)ix} [(\dot{x}_{(i+1)} - \dot{x}_i) - b_{iu}(\dot{\psi}_{(i+1)} - \dot{\psi}_i) + c_{iu}(\dot{\varphi}_{(i+1)} - \dot{\varphi}_i)] + \dots \\ &\quad + k_{(i+1)ix} [(x_{(i+1)} - x_i) - b_{iu}(\psi_{(i+1)} - \psi_i) + c_{iu}(\varphi_{(i+1)} - \varphi_i)] \end{aligned} \quad (2.2)$$

— along the y -axis

$$\begin{aligned} F_{i(i-1)y} &= d_{i(i-1)y} [-(\dot{y}_i - \dot{y}_{(i-1)}) + a_{id}(\dot{\psi}_i - \dot{\psi}_{(i-1)}) + c_{id}(\dot{\theta}_i - \dot{\theta}_{(i-1)})] + \dots \\ &\quad + k_{i(i-1)y} [-(y_i - y_{(i-1)}) + a_{id}(\psi_i - \psi_{(i-1)}) + c_{id}(\theta_i - \theta_{(i-1)})] \\ F_{(i+1)iy} &= d_{(i+1)iy} [(\dot{y}_{(i+1)} - \dot{y}_i) + a_{iu}(\dot{\psi}_{(i+1)} - \dot{\psi}_i) - c_{iu}(\dot{\theta}_{(i+1)} - \dot{\theta}_i)] + \dots \\ &\quad + k_{(i+1)iy} [(y_{(i+1)} - y_i) + a_{iu}(\psi_{(i+1)} - \psi_i) - c_{iu}(\theta_{(i+1)} - \theta_i)] \end{aligned} \quad (2.3)$$

— along the z -axis

$$\begin{aligned}
 F_{i(i-1)z} &= d_{i(i-1)z}[-(\dot{z}_i - \dot{z}_{(i-1)}) - a_{id}(\dot{\varphi}_i - \dot{\varphi}_{(i-1)}) + b_{id}(\dot{\theta}_i - \dot{\theta}_{(i-1)})] + \dots \\
 &\quad + k_{i(i-1)z}[-(z_i - z_{(i-1)}) - a_{id}(\varphi_i - \varphi_{(i-1)}) + b_{id}(\theta_i - \theta_{(i-1)})] \\
 F_{(i+1)iz} &= d_{(i+1)iz}[(\dot{z}_{(i+1)} - \dot{z}_i) - a_{iu}(\dot{\varphi}_{(i+1)} - \dot{\varphi}_i) + b_{iu}(\dot{\theta}_{(i+1)} - \dot{\theta}_i)] + \dots \\
 &\quad + k_{(i+1)iz}[(z_{(i+1)} - z_i) - a_{iu}(\varphi_{(i+1)} - \varphi_i) + b_{iu}(\theta_{(i+1)} - \theta_i)]
 \end{aligned} \tag{2.4}$$

where $d_{i(i-1)j}$, $d_{(i+1)iz}$ and $k_{i(i-1)z}$, $k_{(i+1)iz}$ are the damping and stiffness coefficients which represent visco-elastic connections between neighbouring bodies ($i = 1, 2, 3$) in the specific direction $j = x, y, z$ of the vibration exposure, a_{id} , a_{iu} , b_{id} , b_{iu} , c_{id} , c_{iu} are the distances defining fixations of the lower (index u) and upper (index d) visco-elastic elements to particular bodies. The above equations (Eqs. (2.2)-(2.4)) take into account the linear displacements of individual masses as well as their possible rotations around each axis. Assuming relatively small torsional movements, the angular displacements are approximated by corresponding values of the angles θ_i , φ_i and ψ_i .

The force F_{2x} representing contact of the human body with the seat backrest as well as the active force F_{sky} stabilising the head are defined in the following way

$$F_{2x} = -d_{2x}(\dot{x}_2 - \dot{x}_0) - k_{2x}(x_2 - x_0) \quad F_{sky} = -d_{sky}\dot{y}_3 \tag{2.5}$$

where d_{2x} , k_{2x} are the damping and stiffness coefficients of the backrest, d_{sky} is the sky-hook damping ratio that reproduce the human action against vibration.

The next set of equations describe the angular motion of particular bodies around particular axes

$$\begin{aligned}
 J_{ix}\ddot{\theta}_i &= -F_{i(i-1)y}c_{id} - F_{i(i-1)z}b_{id} - F_{(i+1)iy}c_{iu} + F_{(i+1)iz}b_{iu} \\
 J_{iy}\ddot{\varphi}_i &= F_{i(i-1)x}c_{id} + F_{i(i-1)z}a_{id} + F_{(i+1)ix}c_{iu} - F_{(i+1)iz}a_{iu} \\
 J_{iz}\ddot{\psi}_i &= F_{i(i-1)x}b_{id} - F_{i(i-1)y}a_{id} - F_{(i+1)ix}b_{iu} + F_{(i+1)iy}a_{iu}
 \end{aligned} \quad i = 1, 2, 3 \tag{2.6}$$

where J_{ix} , J_{iy} and J_{iz} are mass moments of inertia for individual body segments ($i = 1, 2, 3$) that are defined around each axis of the Cartesian coordinate system.

3. Measurement and data processing

The experimental set-up for measuring the body motion under vibration in various directions is shown in Fig. 4. The vibration shaker is used to generate random oscillatory motion along three orthogonal directions, i.e. longitudinal x -direction (Fig. 4a), lateral y -direction (Fig. 4b) and vertical z -direction (Fig. 4c). Three-directional accelerometers are mounted to individual human body parts such as pelvis, torso and head. Additionally, the fourth accelerometer is utilised to measure the input vibration source of the shaker providing random vibration with a frequency between 0.5 Hz and 12.5 Hz. The data obtained from accelerators are recorded by a PC-based data acquisition system with the sampling time of 1 ms.

The originally measured acceleration signals are reduced to the sampling frequency of 200 Hz by averaging of every 5 samples and then converted into frequency-domain data. For each signal, the power spectral density (PSD) is computed by employing Welch's method (Stoica and Moses, 2005) with a Hamming window applied to 50% overlapping the segments of the measurement data. The length of each data segment corresponds to the time period of 10.24 s that allows one to achieve a frequency resolution of 97.66 mHz. Based on such prepared frequency-domain data, the vibration transmissibility of particular human body parts are calculated as follows

$$T_{ij}(2\pi f) = \frac{\sqrt{\text{PSD}_{ij}(2\pi f)}}{\sqrt{\text{PSD}_{0j}(2\pi f)}} \quad i = 1, 2, 3 \quad j = x, y, z \tag{3.1}$$

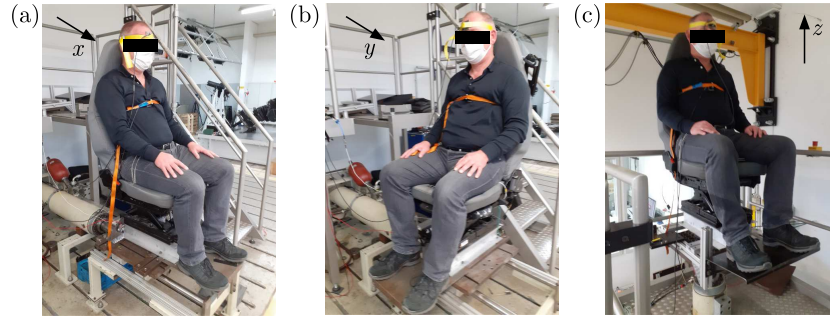


Fig. 4. Experimental set-up for measuring body motion exposed to vibration in different directions: (a) longitudinal x -direction, (b) lateral y -direction, (c) vertical z -direction

where $\text{PSD}_{ij}(2\pi f)$ is the power spectral density of the selected human body part (pelvis $i = 1$, torso $i = 2$ and head $i = 3$), $\text{PSD}_{i0}(2\pi f)$ is the power spectral density of the base vibration that is measured along a specific axis of the vibration transfer (the longitudinal axis $j = x$, lateral axis $j = y$ and vertical axis $j = z$), f is the frequency in Hz.

A scalar transmissibility function (Eq. (3.1)) is therefore estimated via PSD as a ratio between two measured signals, i.e. the base vibration and vibration of the selected human body part. If a magnitude of the transmissibility function is below 1, then the desired vibration reduction is achieved. Otherwise, the unwanted amplification of a vibration magnitude is observed due to resonances of the human body parts and organs.

4. Identification of model parameters

The identification of model parameters is conducted by minimising the root mean square error (RMSE) of the transmissibility function determined above. Such a procedure is realised in the following way

$$\text{RMSE} = \sum_{i=1}^3 \sum_{j=x}^z \sqrt{\frac{1}{N} \sum_{n=1}^N [T_{ij}(2\pi f_n) - \hat{T}_{ij}(2\pi f_n)]^2} \quad \begin{array}{l} i = 1, 2, 3 \\ j = x, y, z \end{array} \quad (4.1)$$

where T_{ij} and \hat{T}_{ij} are magnitudes of the simulated and measured transmissibility functions, respectively, that correspond to the frequency vector f_n of N -elements. The proposed identification method accepts fitting of more than one transmissibility function evaluated for individual human body parts ($i = 1, 2, 3$) and along various directions ($j = x, y, z$) of the vibration transmission.

Assuming the averaged masses m_1 , m_2 and m_3 of the particular human body parts (Chandler *et al.*, 1975) as well as their mass moments of inertia J_{1j} , J_{2j} and J_{3j} around different axes ($j = x, y, z$ – see Appendix), the objective function to be minimised is defined as follows

$$\min_{d_{i(i-1)j}, k_{i(i-1)j}, d_{2x}, k_{2x}, d_{sky}} \text{RMSE}(d_{i(i-1)j}, k_{i(i-1)j}, d_{2x}, k_{2x}, d_{sky}) \quad \begin{array}{l} i = 1, 2, 3 \\ j = x, y, z \end{array} \quad (4.2)$$

where $d_{i(i-1)j}$ and $k_{i(i-1)j}$ are the damping and stiffness coefficients determining visco-elastic interactions between individual masses of the bio-mechanical model, d_{2x} and k_{2x} are the damping and stiffness coefficients representing the transmission of fore-aft vibration through the seat backrest (only in the longitudinal x -direction), d_{sky} is the damping coefficient describing active stabilisation of the head due to the human body's ability to absorb vibrational energy (only in the lateral y -direction). The block diagram for identification of the unknown model parameters is presented in Fig. 5.

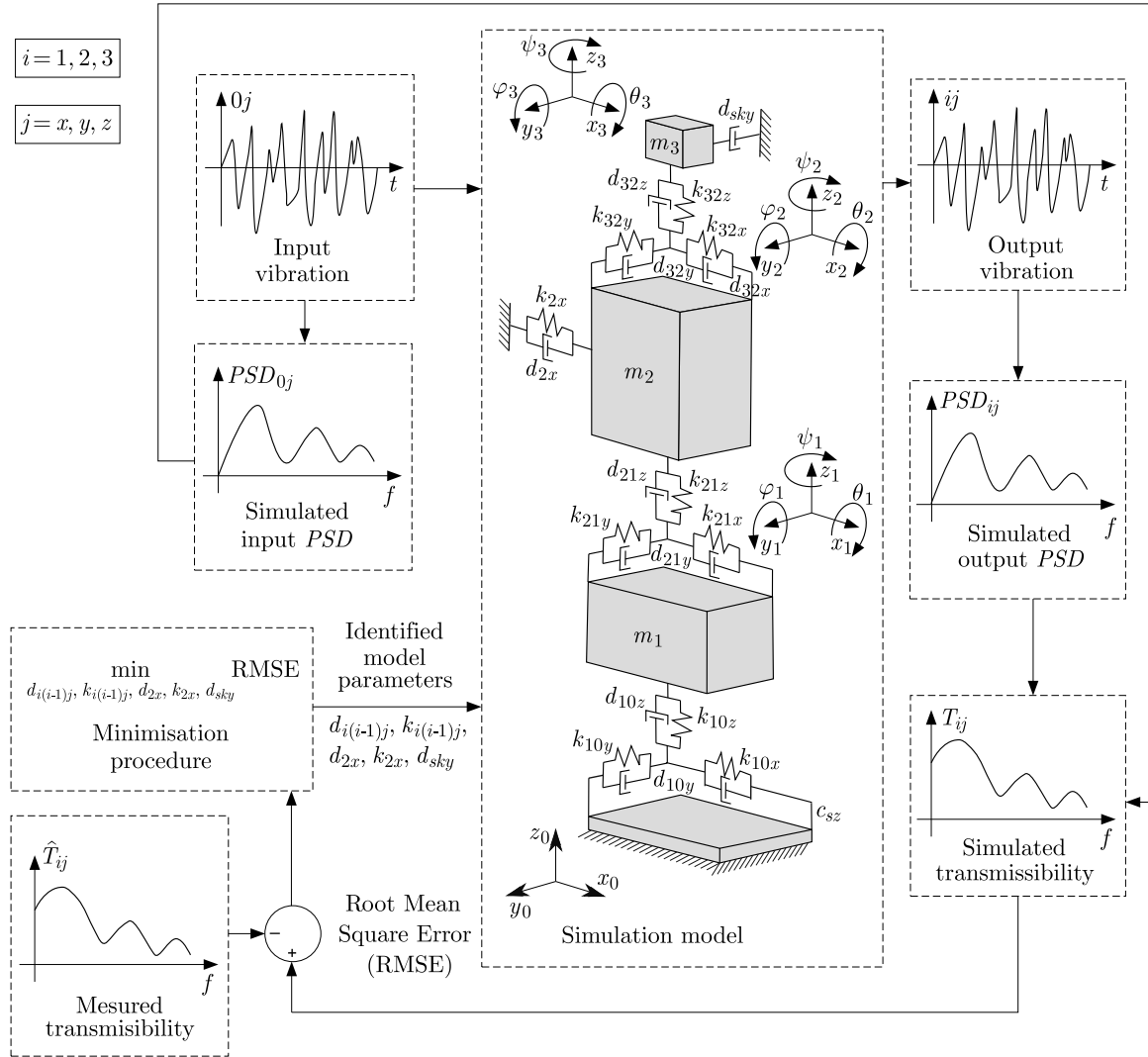


Fig. 5. Block diagram for identification of the unknown model parameters

For the reason of finding a minimum of the objective function (Eq. (4.2)) of several variables, the gradient method is utilised. Such a method is implemented in the MATLAB® environment and can be employed for searching an optimal configuration of the unknown damping and stiffness coefficients that have a significant influence on the model output. The initial estimate of these parameters plays an important role in minimising the error between the simulation and measurement results, therefore the proposed optimisation procedure is repeated many times by using a large number of random starting points. The optimal model parameters that conform to a global minimum of the RMSE are shown in Table 1. As follows from this table, if the stiffness and damping coefficients are equal to zero along some axis (x, y or z) then the vibration transmission of a model does not occur for these directions. The obtained results are strictly connected with a specific geometrical configuration of the bio-mechanical model that depends on the complete set of its dimensions such as $a_{id}, a_{iu}, b_{id}, b_{iu}$ and c_{id}, c_{iu} ($i = 1, 2, 3$) – see Appendix.

5. Simulation and experimental results

The bio-mechanical model discussed within the framework of this paper is investigated by means of a numerical simulation and an experimental research under laboratory conditions. The male subject of 90 kg is employed for measurements of the seated human body exposed to whole-body

Table 1. Identified model parameters for different directions of the input vibration

Parameter	Input vibration			Unit
	along x -axis	along y -axis	along z -axis	
d_{10x}	23.58	0	6711	Ns/m
k_{10x}	27507	0	10.13	N/m
d_{10y}	0	24069	0	Ns/m
k_{10y}	0	171570	0	N/m
d_{10z}	10000	0	1525	Ns/m
k_{10z}	82931	0	14222	N/m
d_{21x}	38.13	0	1.04	Ns/m
k_{21x}	27646	0	16094	N/m
d_{21y}	0	10	0	Ns/m
k_{21y}	0	8522	0	N/m
d_{21z}	2619	0	1266	Ns/m
k_{21z}	6126	0	66258	N/m
d_{32x}	50	0	85.65	Ns/m
k_{32x}	3418	0	16860	N/m
d_{32y}	0	2487	0	Ns/m
k_{32y}	0	63442	0	N/m
d_{32z}	2404	0	1325	Ns/m
k_{32z}	500	0	24584	N/m
d_{2x}	10	0	1684	Ns/m
k_{2x}	8045	0	62046	N/m
d_{sky}	0	35.51	0	Ns/m

vibration. The laboratory examination of the human dynamics are executed according to the International Standard ISO-7096 (2000) that rigorously defines the person posture on a seat as well as experimental instrumentation of the test rig (Fig. 4). The signals acquired from 3D linear accelerometers measuring acceleration of the input vibration together with accelerations of the particular human body parts (pelvis, torso and head) are used for further analysis. Based on these signals, the transmissibility functions (Eq. (3.1)) are evaluated and compared with the results obtained by computer simulation in the studied frequency range of 0.5 Hz to 12.5 Hz (Fig. 6).

As shown in Fig. 6, the proposed model demonstrates good agreement with the measurement results. The bio-dynamic response of the seated human body is captured in various directions of the vibration influence even if the input vibration is generated along a single axis (vibration generated along the longitudinal x -direction – Fig. 6a,b and vibration generated along the vertical z -direction – Fig. 6d,e). Exception to this rule is observed when vibration is generated along the lateral y -direction – Fig. 6c. Due to system symmetry around the z -axis, only the lateral vibration response of both simulation model and human subject is shown. Note that other geometrical configurations of the bio-mechanical model can produce its dynamic response along various axes (x , y and/or z) of the three-dimensional coordinate system.

Considering the system configuration depicted in Appendix , the transmissibility functions for the input vibration applied in the x -direction are illustrated in Fig. 6a,b. There is a significant increase of the vibration that are transferred from the human pelvis to the head (through the torso) in both directions of the vibration transmission, i.e. from the x -direction to x -direction (Fig. 6a) and also from the x -direction to z -direction (Fig. 6b). In turn, an application of the input vibration in the y -direction (Fig. 6c) results in a different dynamic response of the vibrating system. The torso points out high magnitudes of vibration at low frequencies and the

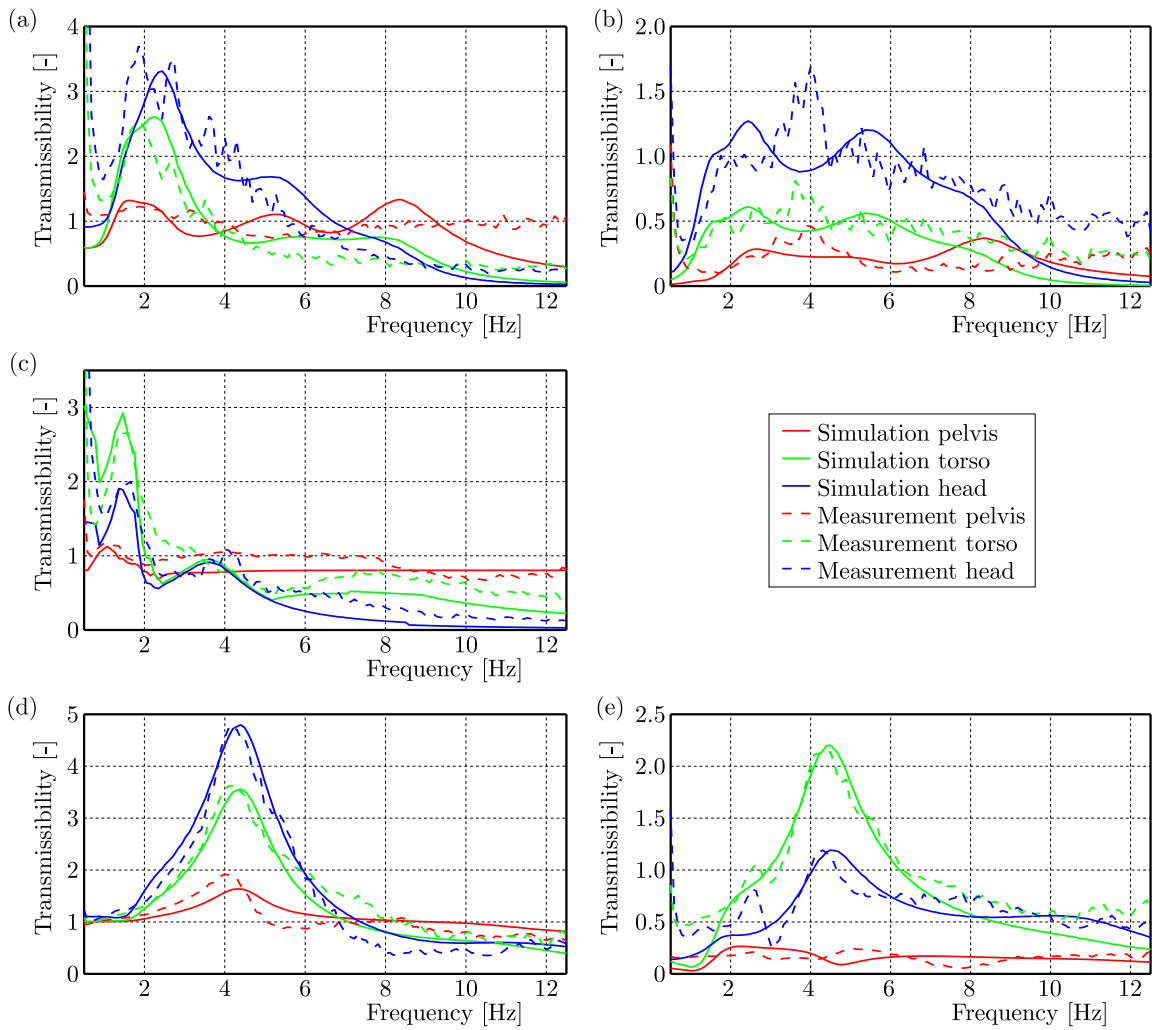


Fig. 6. Transmissibility functions of the human body obtained for different directions of the vibration exposure from: (a) x -direction to x -direction, (b) x -direction to z -direction, (c) y -direction to y -direction, (d) z -direction to z -direction, (e) z -direction to x -direction

Table 2. RMS accelerations of different human body parts obtained by means of computer simulation and laboratory measurement

Output vibration	Human body part	Input vibration					
		along x -direction		along y -direction		along z -direction	
		RMS acceleration [m/s^2]					
		simulation	experiment	simulation	experiment	simulation	experiment
x -direction	Pelvis	1.488	1.451	0	0.149	0.354	0.333
	Torso	1.607	1.555	0	0.112	1.387	1.412
	Head	2.449	2.544	0	0.170	0.846	0.883
y -direction	Pelvis	0	0.189	1.289	1.370	0	0.182
	Torso	0	0.163	1.429	1.410	0	0.151
	Head	0	0.161	1.151	1.241	0	0.194
z -direction	Pelvis	0.354	0.311	0	0.169	1.528	1.468
	Torso	0.529	0.561	0	0.137	2.377	2.403
	Head	1.042	1.148	0	0.175	2.852	2.796

head vibration is actively reduced by the human due to enlarged postural control. Subsequently, the vibration input in the z -direction (Fig. 6d,e) leads to an increase in vibration transmission by individual parts of the human body, i.e. from the pelvis through the torso to the head, but this phenomenon is observed only along the vertical axis (Fig. 6d). Similarly to the previous direction of excitation, the human head shows lower magnitudes while vibration is transferred from the vertical z -direction to the longitudinal x -direction (Fig. 6e).

The presented results well represent the dependence of human sensitivity to vibration in terms of frequency. According to ISO-2631 (1997), the most dangerous range of frequencies for horizontal vibration is between 0.5 Hz and 3 Hz (Figs. 6a and 6c) and for vertical vibration, the frequency ranges from 4 Hz to 8 Hz (Fig. 6d), because several body eigenfrequencies of the seated human are included within these scopes. The root mean square (RMS) accelerations of different human body parts, which are obtained by means of computer simulation and laboratory measurement, are listed in Table 2. Notice that the simulated RMS accelerations equal to 0 m/s² mean that no vibration transmission across the selected axes is obtained. Even then the measured RMS accelerations have low values as a result of the measurement noise.

6. Conclusions

In the paper, a simplified model of the human body is proposed and investigated by means of experimental tests under laboratory conditions. The presented model reproduces the dynamic spatial response of a seated human subject to harmful vibration even if the model input is selected as a single-axis excitation. The application of such a model leads to better prediction of human reactions to the whole-body vibration than in commonly used uniaxial models. The input vibration energy is transferred via the human body in various directions simultaneously, which results in a reduction of vibration amplitudes measured along the axis compliant with the excitation direction. As follows from the results shown in this paper, the recommended model is helpful for explaining and predicting human behaviour in a vibrational environment and can be satisfactorily used for simulation purposes of the seating dynamics. A developed simulation model of the human body will be combined with the seat suspension system in further research. The passive and active suspension systems of various mechanical structures will be investigated in order to decrease the harmful influence of mechanical vibrations on humans.

Appendix – Constant model parameters of the seated human body

Parameter	Value	Unit
Masses of individual body parts		
Pelvis (m_1)	25.18	kg
Torso (m_2)	46.77	kg
Head (m_3)	8.04	kg
Mass moments of inertia around different axes		
Pelvis around longitudinal axis (J_{1x})	0.3659	kg·m ²
Pelvis around lateral axis (J_{1y})	0.6650	kg·m ²
Pelvis around vertical axis (J_{1z})	0.9705	kg·m ²
Torso around longitudinal axis (J_{2x})	1.412	kg·m ²
Torso around lateral axis (J_{2y})	1.032	kg·m ²
Torso around vertical axis (J_{2z})	0.867	kg·m ²
Head around longitudinal axis (J_{3x})	0.0871	kg·m ²
Head around lateral axis (J_{3y})	0.1020	kg·m ²

Head around vertical axis (J_{3z})	0.0687	kg·m ²
Dimensions for mounting visco-elastic elements		
Pelvis along longitudinal axis – lower fixation (a_{1d})	0	m
Pelvis along lateral axis – lower fixation (b_{1d})	0	m
Pelvis along vertical axis – lower fixation (c_{1d})	0.06	m
Pelvis along longitudinal axis – upper fixation (a_{1u})	-0.15	m
Pelvis along lateral axis – upper fixation (b_{1u})	0	m
Pelvis along vertical axis – upper fixation (c_{1u})	0.06	m
Torso along longitudinal axis – lower fixation (a_{2d})	0	m
Torso along lateral axis – lower fixation (b_{2d})	0	m
Torso along vertical axis – lower fixation (c_{2d})	0.225	m
Torso along longitudinal axis – upper fixation (a_{2u})	-0.025	m
Torso along lateral axis – upper fixation (b_{2u})	0	m
Torso along vertical axis – upper fixation (c_{2u})	0.225	m
Head along longitudinal axis – lower fixation (a_{3d})	-0.045	m
Head along lateral axis – lower fixation (b_{3d})	0	m
Head along vertical axis – lower fixation (c_{3d})	0.15	m

Acknowledgements

We would like to thank Isringhausen GmbH and Co. KG for the assistance in the experimental research.

References

- ADAM S.A., JALIL N.A.A., 2017, Vertical suspension seat transmissibility and SEAT values for seated person exposed to whole-body vibration in agricultural tractor – preliminary study, *Procedia Engineering*, **170**, 435-442
- CHANDLER R.F., CLAUSER C.E, MCCONVILLE J.T., REYNOLDS H.M., 1975 *Investigation of Inertial Properties of the Human Body*, U.S. Department of Transportation within the Project: Seat Design, Driver Comfort, and the Automotive Package, Washington
- DESAI R., GUHA A., SESHU P., 2018, Multibody biomechanical modelling of human body response to direct and cross axis vibration, *Procedia Computer Science*, **133**, 494-501
- FRITZ M., 19981, Analyse der vertikalen Auflagenkraft bei unterschiedlichen Sprüngen anhand von gemessenen und simulierten Kraftkurven, *Leistungssport*, **11**, 1, 74-78
- GŁOWIŃSKI S., BLAŻEJEWSKI A., KRÓLIKOWSKI T., KNITTER R., 2019, Gait recognition: a challenging task for MEMS signal identification, *Sustainable Design and Manufacturing*, **155**, 473-483
- GŁOWIŃSKI S., BLAŻEJEWSKI A., KRZYŻYŃSKI T., 2017a, Human gait feature detection using inertial sensors wavelets, *Wearable Robotics: Challenges and Trends – Part of the Biosystems and Biorobotics*, **16**, 397-401
- GŁOWIŃSKI S., BLAŻEJEWSKI A., KRZYŻYŃSKI T., 2017b, Inertial sensors and wavelets analysis as a tool for pathological gait identification, *Innovations in Biomedical Engineering – Part of the Advances in Intelligent Systems and Computing*, **526**, 106-114
- GŁOWIŃSKI S., BLAŻEJEWSKI A., KRZYŻYŃSKI T., 2018, Body part accelerations evaluation for chosen techniques in martial arts, *Advances in Intelligent Systems and Computing*, **623**, 235-243
- GŁOWIŃSKI S., KRZYŻYŃSKI T., PECOLT S., MACIEJEWSKI I., 2015, Design of motion trajectory of an arm exoskeleton, *Archive of Applied Mechanics*, **85**, 75-87

10. International Organization for Standardization ISO 2631, 1997, *Mechanical Vibration and Shock – Evolution of Human Exposure to Whole Body Vibration*, Geneva
11. International Organization for Standardization ISO 7096, 2000, *Earth-Moving Machinery – Laboratory Evaluation of Operator Seat Vibration*, Geneva
12. KIM T.H., KIM Y.T., YOON Y.S., 2005, Development of a biomechanical model of the human body in a sitting posture with vibration transmissibility in the vertical direction, *International Journal of Industrial Ergonomics*, **35**, 9, 817-829
13. LIU C., QIU Y., 2020, Localised apparent masses over the interface between a seated human body and a soft seat during vertical whole-body vibration, *Journal of Biomechanics*, **109**, ID 109887, 1-12
14. LIU C., QIU Y., 2021, Mechanism associated with the effect of backrest inclination on biodynamic responses of the human body sitting on a rigid seat exposed to vertical vibration, *Journal of Sound and Vibration*, **510**, ID 116299, 1-22
15. MACIEJEWSKI I., BLAZEJEWSKI A., PECOLT S., KRZYZYNSKI T., 2022, A sliding mode control strategy for active horizontal seat suspension under realistic input vibration, *Journal of Vibration and Control*, **29**, 11-12, 2539-2551
16. MACIEJEWSKI I., KRZYZYNSKI T., 2020, Global sensitivity analysis in optimisation of the vibration reduction systems, *AIP Conference Proceedings*, **2239**, 020028
17. MACIEJEWSKI I., KRZYZYNSKI T., MEYER L., MEYER H., 2017, Shaping the vibro-isolation properties of horizontal seat suspension, *Journal of Low Frequency Noise, Vibration and Active Control*, **36**, 3, 203-213
18. MACIEJEWSKI I., KRZYŻYŃSKI T., PECOLT S., CHAMERA S., 2019, Semi-active vibration control of horizontal seat suspension by using magneto-rheological damper, *Journal of Theoretical and Applied Mechanics*, **57**, 2, 411-420
19. MANDAPURAM S., RAKHEJA S., MARCOTTE P., BOILEAU P.E., 2011, Analyses of biodynamic responses of seated occupants to uncorrelated fore-aft and vertical whole-body vibration, *Journal of Sound and Vibration*, **330**, 16, 4064-4079
20. MIHCIN S., KOSE H., CIZMECIOGULLARI S., CIKLACANDIR S., KOCAK M., TOSUN A., AKAN A., 2019, Investigation of wearable motion capture system towards biomechanical modelling, *IEEE International Symposium on Medical Measurements and Applications*, 1-5
21. SHIPPEN J., MAY B., 2016, BoB – biomechanics in MATLAB, *Proceedings of the 11th International Conference BIOMDLURE*,
22. STEIN G.J., MČKA P., GUNSTON T.P., BADURA S., 2008, Modelling and simulation of locomotive driver's seat vertical suspension vibration isolation system, *International Journal of Industrial Ergonomics*, **38**, 5-6, 384-395
23. STOICA P., MOSES R., 2005, *Spectral Analysis of Signals*, Prentice Hall, New Jersey
24. SUN X., JING X., 2016, A nonlinear vibration isolator achieving high-static-low dynamic stiffness and tunable anti-resonance frequency band, *Mechanical Systems and Signal Processing*, **80**, 166-188
25. SUN S., YANG J., DENG H., DU H., LI W.H., NAKANO M., 2015, Horizontal vibration reduction of a seat suspension using negative changing stiffness magnetorheological elastomer isolators, *International Journal of Vehicle Design*, **68**, 104-118
26. ZHAO Y., ALASHMORI M., BI F., WANG X., 2021, Parameter identification and robust vibration control of a truck driver's seat system using multi-objective optimization and genetic algorithm, *Applied Acoustics*, **173**, ID 107697, 1-13
27. ZHENG G., QIU, Y., GRIFFIN M.J., 2011, An analytic model of the in-line and cross-axis apparent mass of the seated human body exposed to vertical vibration with and without a backrest, *Journal of Sound and Vibration*, **330**, 26, 6509-6525